

LA-UR-21-23167

Approved for public release; distribution is unlimited.

Title: X-ray and Neutron Phase Contrast Imaging at LANL

Author(s): Montgomery, David

Intended for: internal meeting at LANL

Issued: 2021-04-02

Disclaimer:

Los Alamos National Laboratory, an affirmative action/equal opportunity employer, is operated by Triad National Security, LLC for the National Nuclear Security Administration of U.S. Department of Energy under contract 89233218CNA000001. By approving this article, the publisher recognizes that the U.S. Government retains nonexclusive, royalty-free license to publish or reproduce the published form of this contribution, or to allow others to do so, for U.S. Government purposes. Los Alamos National Laboratory requests that the publisher identify this article as work performed under the auspices of the U.S. Department of Energy. Los Alamos National Laboratory strongly supports academic freedom and a researcher's right to publish; as an institution, however, the Laboratory does not endorse the viewpoint of a publication or guarantee its technical correctness.

X-ray and Neutron Phase Contrast Imaging at LANL



Physics Café

David S. Montgomery,
Scientist 5, P-4

February 4th, 2021



Managed by Triad National Security, LLC for the U.S. Department of Energy's NNSA

X-ray and Neutron Phase Contrast Imaging at LANL

- Motivation and History
- Theory of phase contrast imaging (geometric optics)
- Applications to ICF capsule characterization
- Dynamic X-ray Phase Contrast Imaging
- Neutron Phase Contrast Imaging using Cold Neutrons at LANSCE
- Quantitative Analysis (Phase Retrieval in various regimes)
- Advertisement for Online PCI Course (two 2 hour sessions)
- Summary and Conclusions

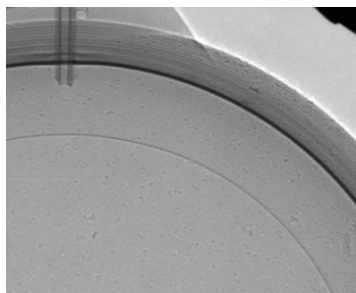
Phase contrast has opened new avenues for x-ray imaging since you don't need absorption for contrast

- for nearly 100 years x-ray imaging relied on absorption to get contrast
- many interesting objects are transparent to x-rays but optically opaque
- propagation-based x-ray phase contrast imaging:
 - does *not* require special optics
 - does *not* require monochromatic x-rays
 - but *does require* sufficient spatial coherence (collimated source, point source)
- x-ray phase contrast imaging relies on wave overlap and interference to produce bright and dark fringes near material density gradients

1896 (absorption)



2005 (phase)

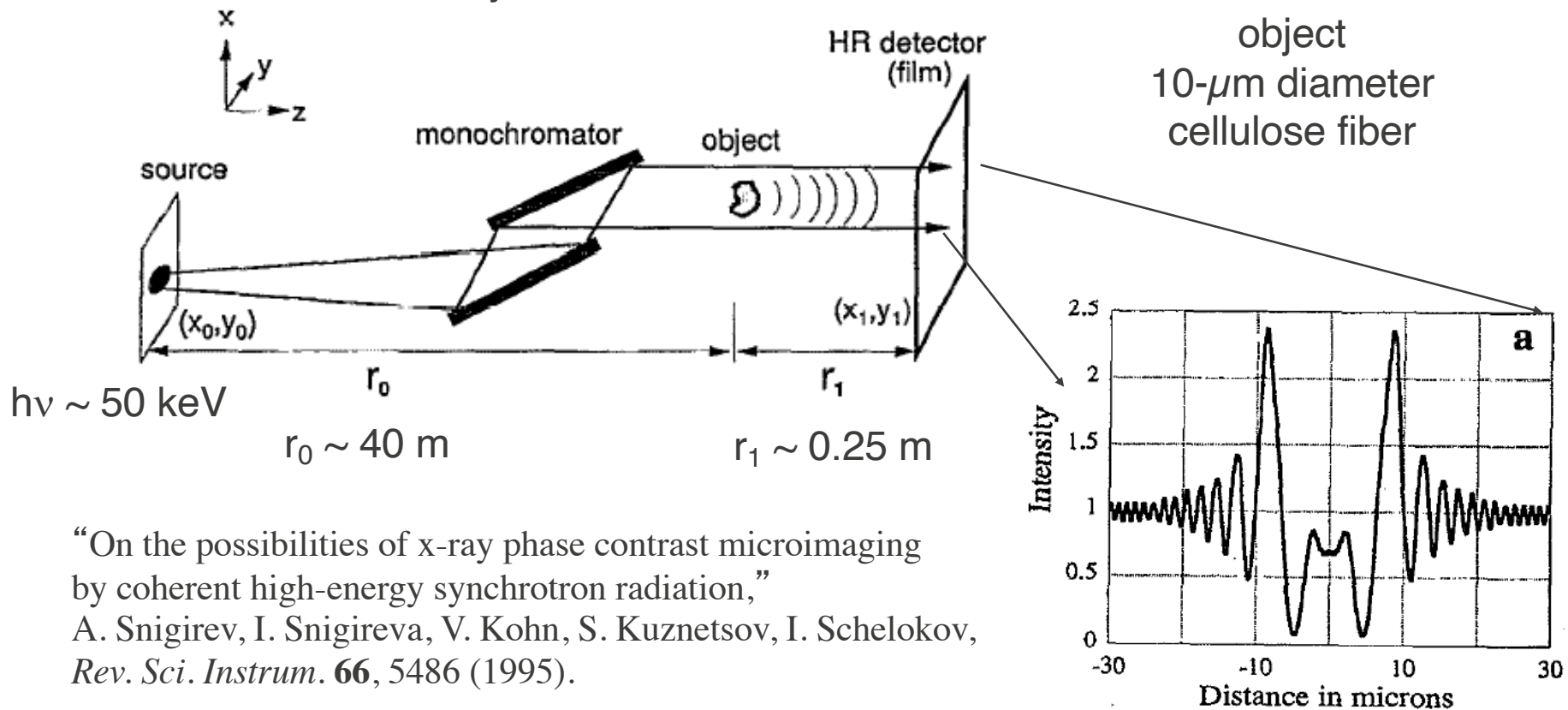


complex index of refraction: $n = 1 - \delta + i\beta$

$$\text{phase: } \varphi = \frac{2\pi}{\lambda} \int (n(x, y, z) - 1) dz \sim \varrho T(x)$$

Propagation-based X-ray phase contrast imaging first observed by Snigirev and co-workers in 1995

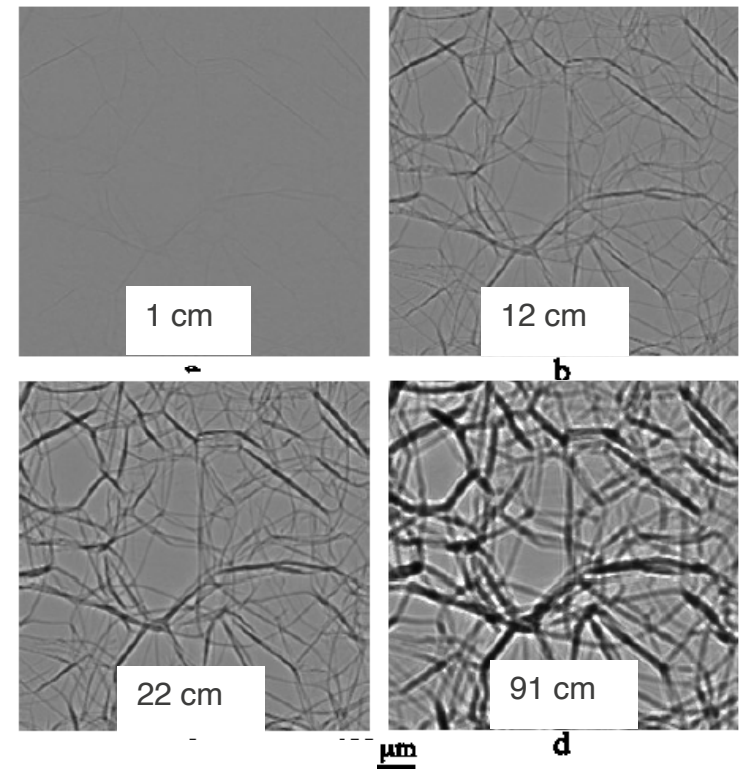
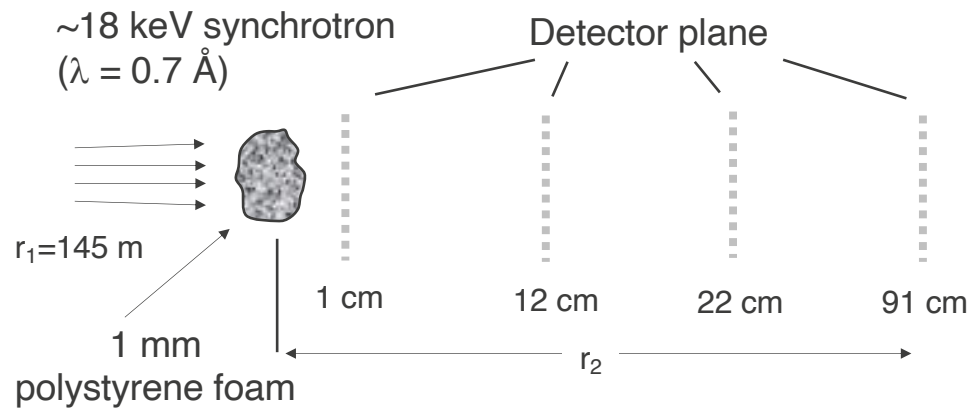
ESRF Synchrotron source



“On the possibilities of x-ray phase contrast microimaging by coherent high-energy synchrotron radiation,”

A. Snigirev, I. Snigireva, V. Kohn, S. Kuznetsov, I. Schelokov, *Rev. Sci. Instrum.* **66**, 5486 (1995).

XPCI produces “high contrast” images for otherwise transparent objects

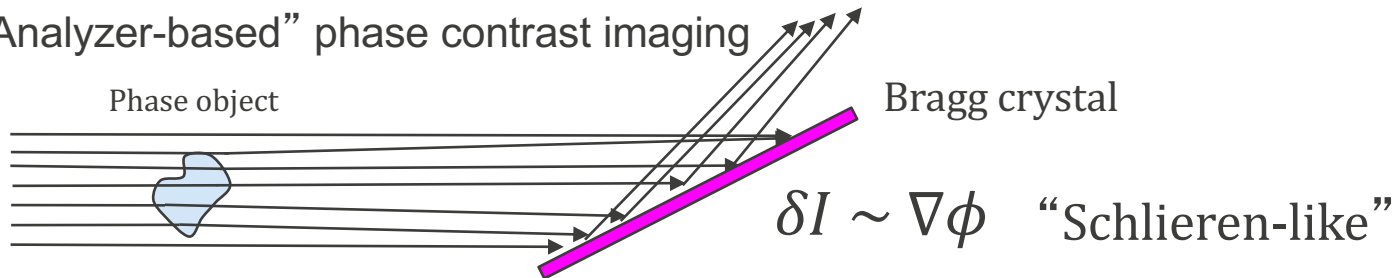


- No contrast observed at $r_2 \sim 0$
- Contrast increases with increasing r_2
- Broadening from diffraction with increasing r_2

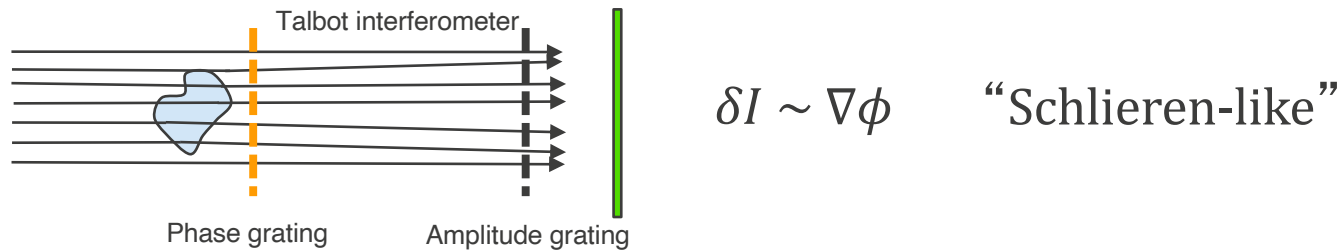
P. Cloetens *et al.*, *J. Phys. D* **32**, A145 (1999)

Various “phase contrast imaging” methods: propagation based method doesn’t require special optics

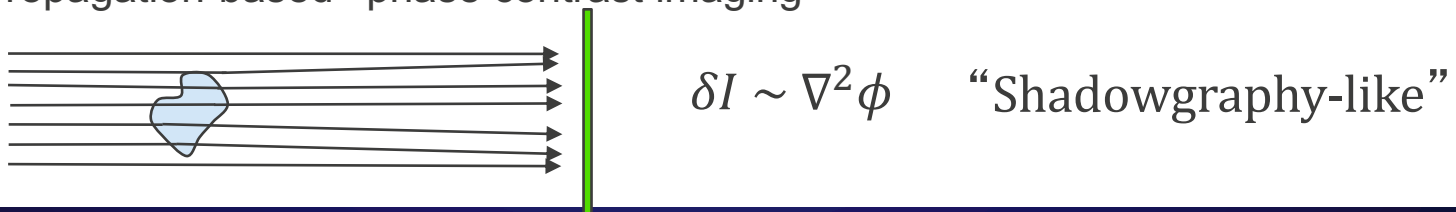
“Analyzer-based” phase contrast imaging



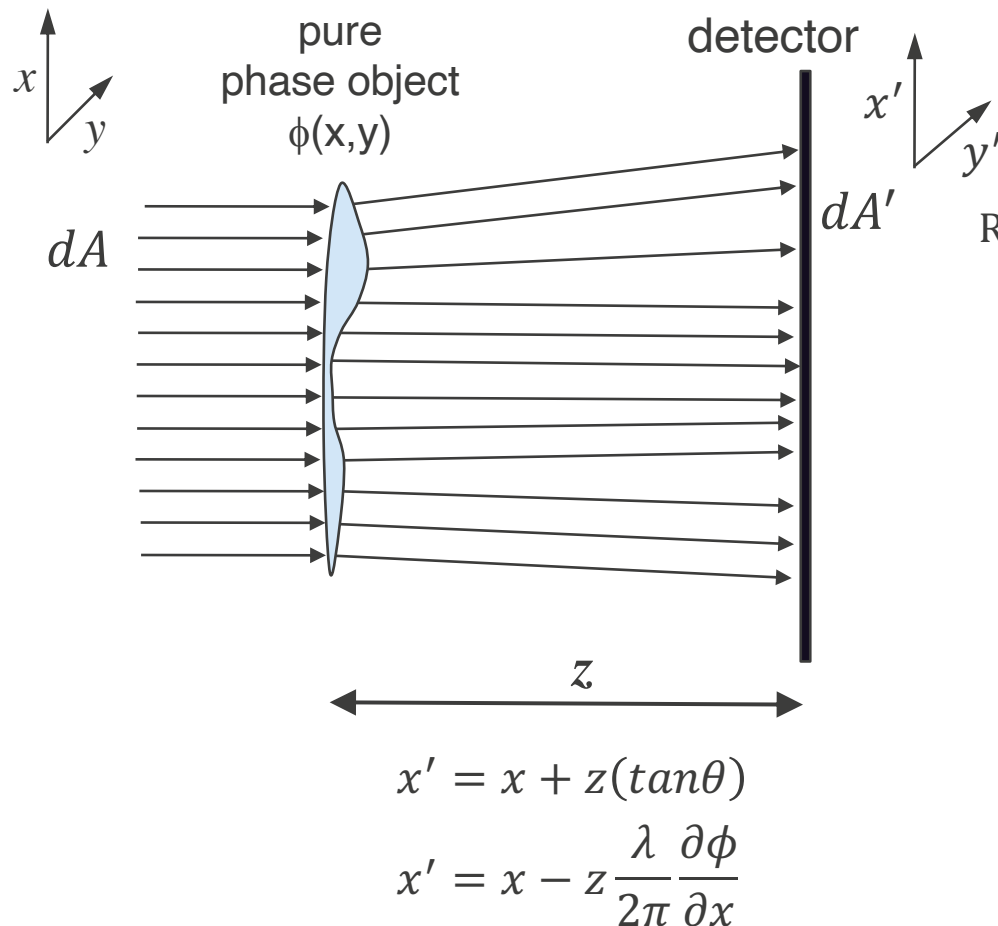
“Grating-based” phase contrast imaging



“Propagation-based” phase contrast imaging



Propagation-Based Phase Contrast Imaging: a Geometric Optics View



mapping of (x, y) to (x', y')
 area dA ($\partial x \partial y$) has area dA' ($\partial x' \partial y'$)

Relative intensity at z is $dA/dA' = \left(\frac{\partial x'}{\partial x} \frac{\partial y'}{\partial y} \right)^{-1}$

$$\frac{\partial x'}{\partial x} = 1 - \frac{\lambda z}{2\pi} \frac{\partial^2 \phi}{\partial x^2}, \quad \frac{\partial y'}{\partial y} = 1 - \frac{\lambda z}{2\pi} \frac{\partial^2 \phi}{\partial y^2}$$

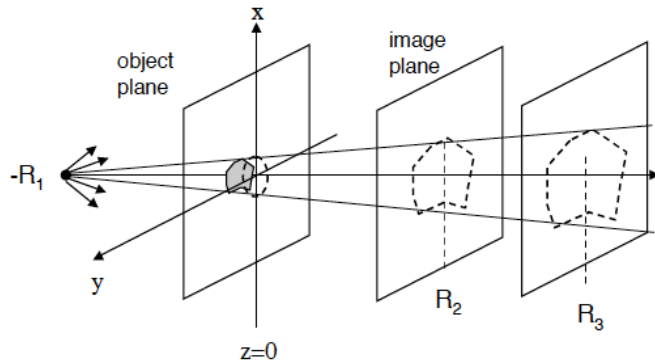
$$I(x', y') = I_0 \left(1 - \frac{\lambda z}{2\pi} \nabla_{\perp}^2 \phi \right)^{-1}$$

in the limit of small argument

$$I(x', y') \approx I_0 \left(1 + \frac{\lambda z}{2\pi} \nabla_{\perp}^2 \phi \right)$$

B. Jensen, D. Montgomery et al. (2019)

Different regimes of propagation are characterized by the dimensionless Fresnel number



Fresnel Number $N_F = a^2 / \lambda z$

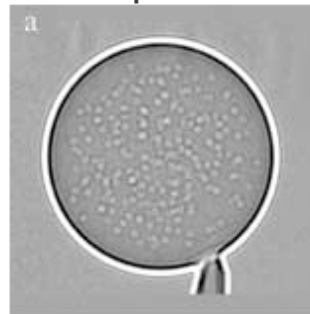
$N_F \gg 1$: geometric optics

$N_F \sim 1$: Fresnel diffraction

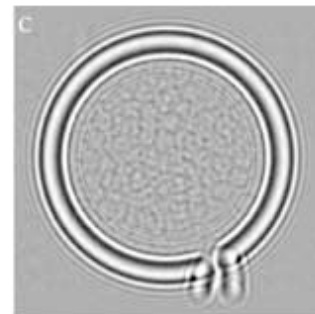
$N_F \ll 1$: Fraunhofer diffraction

from Gureyev *et al* (1999)

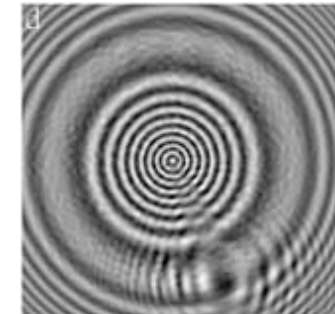
“near-field”
geometric
optics



“intermediate”
Fresnel
diffraction



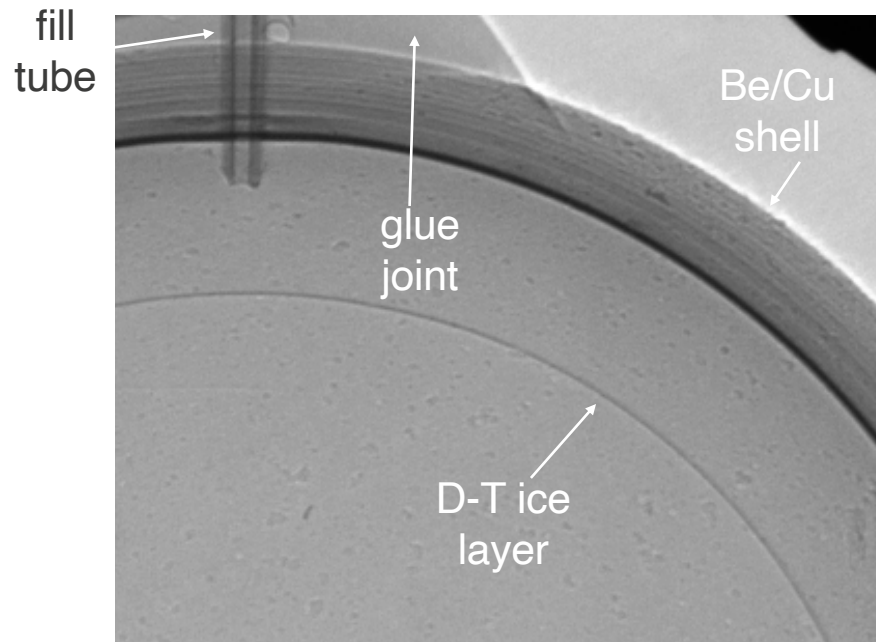
“far-field”
Fraunhofer
Diffraction



all regimes of N_F can be useful for
x-ray phase contrast imaging

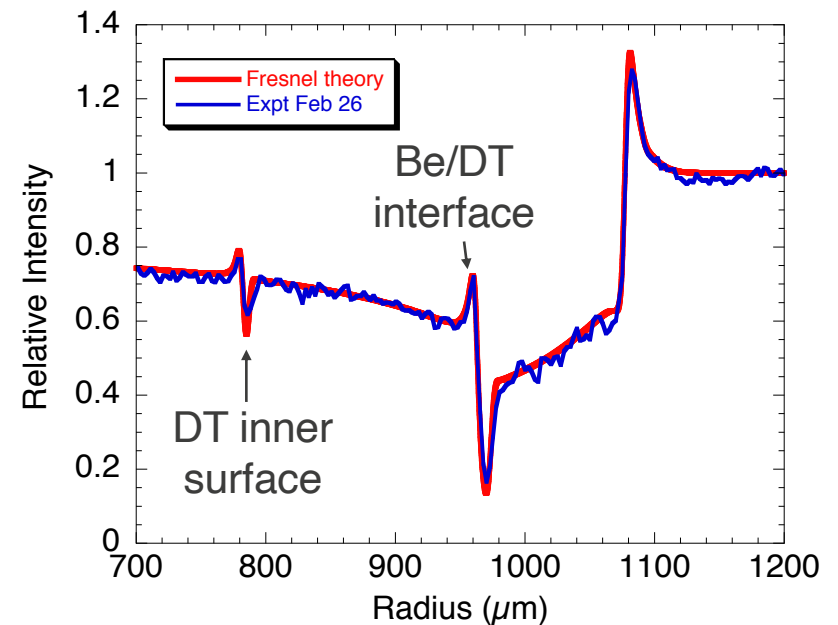
XPCI was further developed by LANL starting in 2004 to characterize cryogenic ICF capsules on NIF

XPCI image of first cryo Be capsule



8 keV Cu K- α , 5- μm spot
 $R_1 = 7.3$ cm, $R_2 = 68.5$ cm, $M = 10.4$
(divergence ~ 70 μrad)

comparison of Fresnel modeling and experimental data

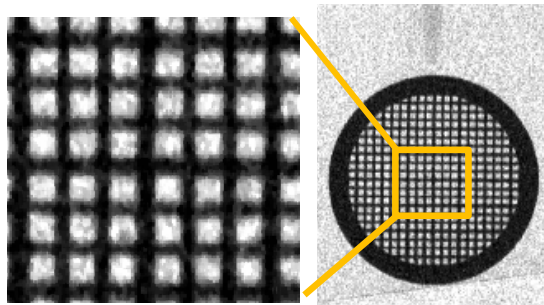


D. Montgomery et al. RSI (2004)
D. Montgomery et al. IFSA (2005)

First ever XPCI in dynamic experiments was demonstrated on Trident using laser-driven blast wave

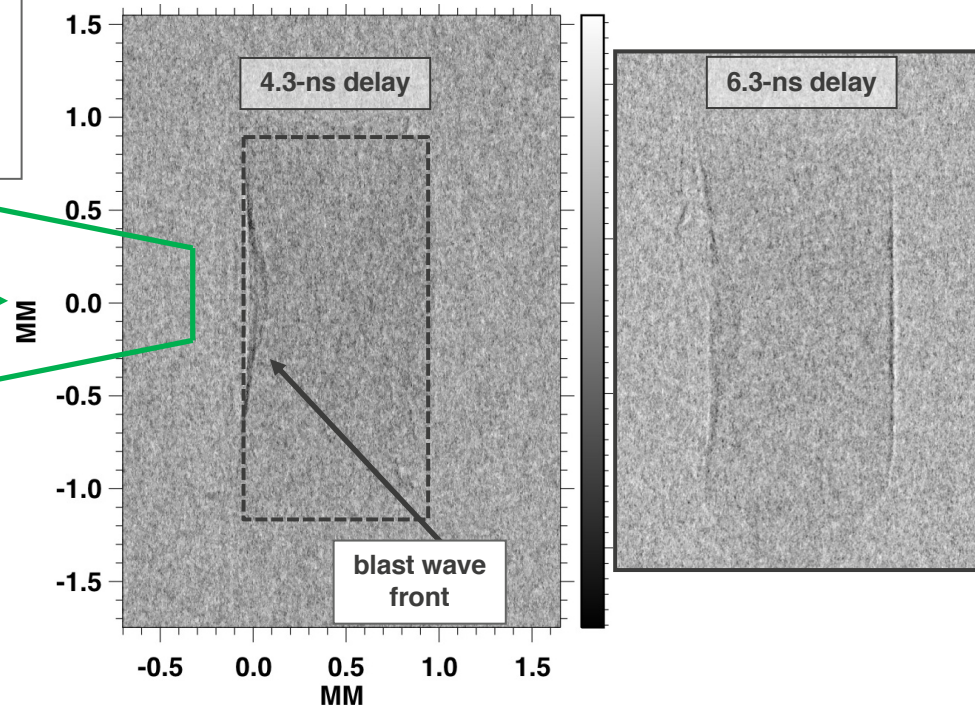
shocked CH (polystyrene) imaged with 17-keV x-rays from 2-ps-driven 10- μ m Mo wire shows refractive effects produced from steep density gradients

2-ns laser drive, 200-J, 527-nm



10/16- μ m grids

17-keV point projection radiography with 10- μ m source



J. Workman *et al*, *RSI* (2010)

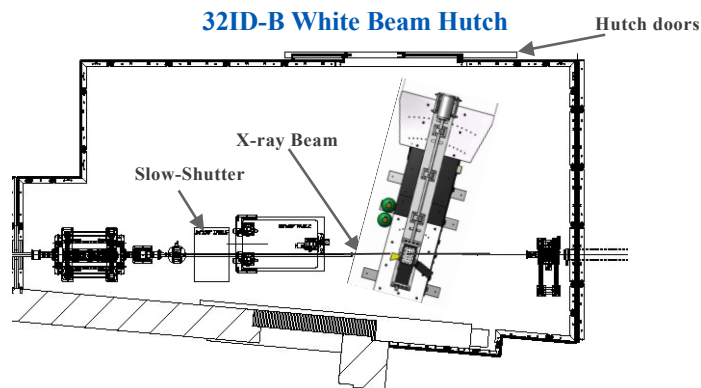
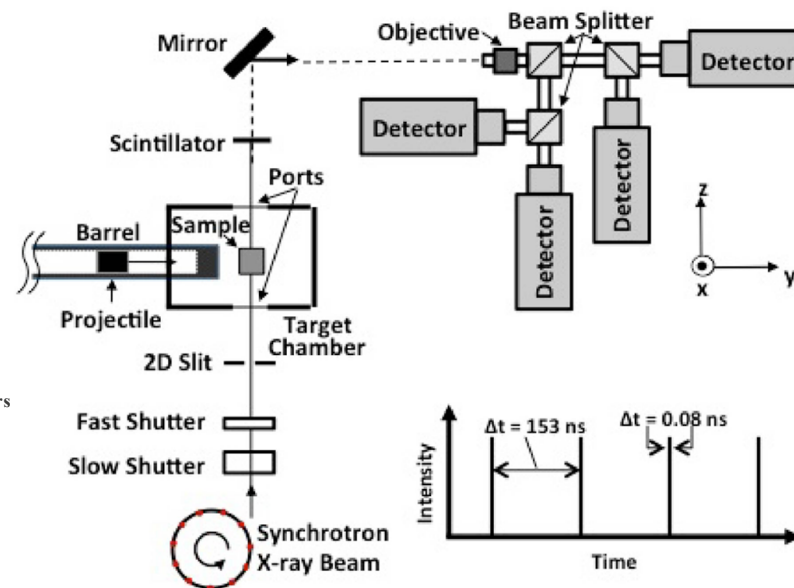
XPCI of dynamic material experiments was pioneered by LANL at the APS synchrotron beginning in 2013

Photo of the Advanced Photon Source (Argonne, IL)

gun located at Sector 32



Experimental arrangement for gas-gun driven experiments using PCI at APS Sector 32

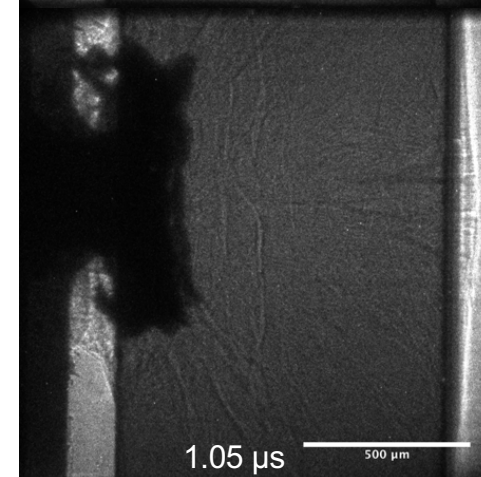
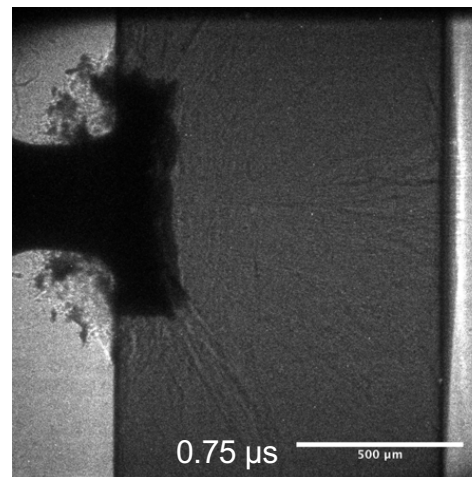
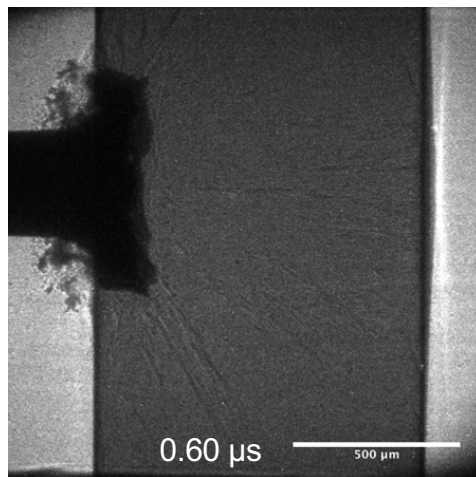
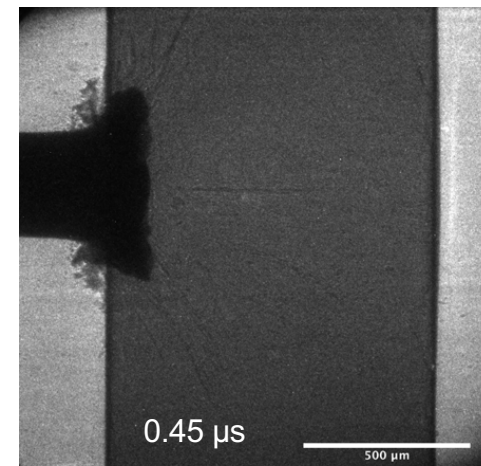
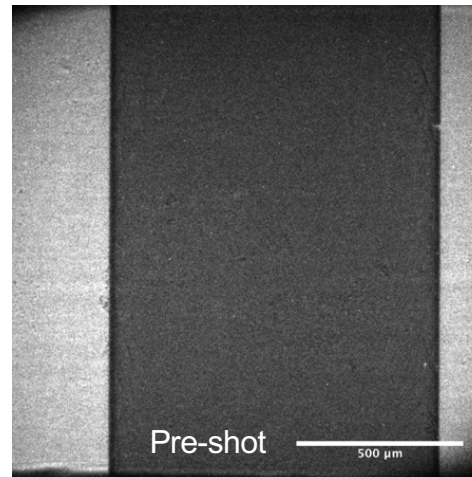
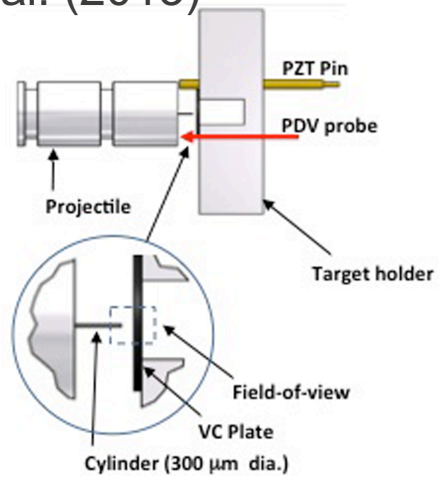


Four PCI images can be obtained using 80-ps duration X-ray pulses provided every 153 ns by the synchrotron operated in the standard mode

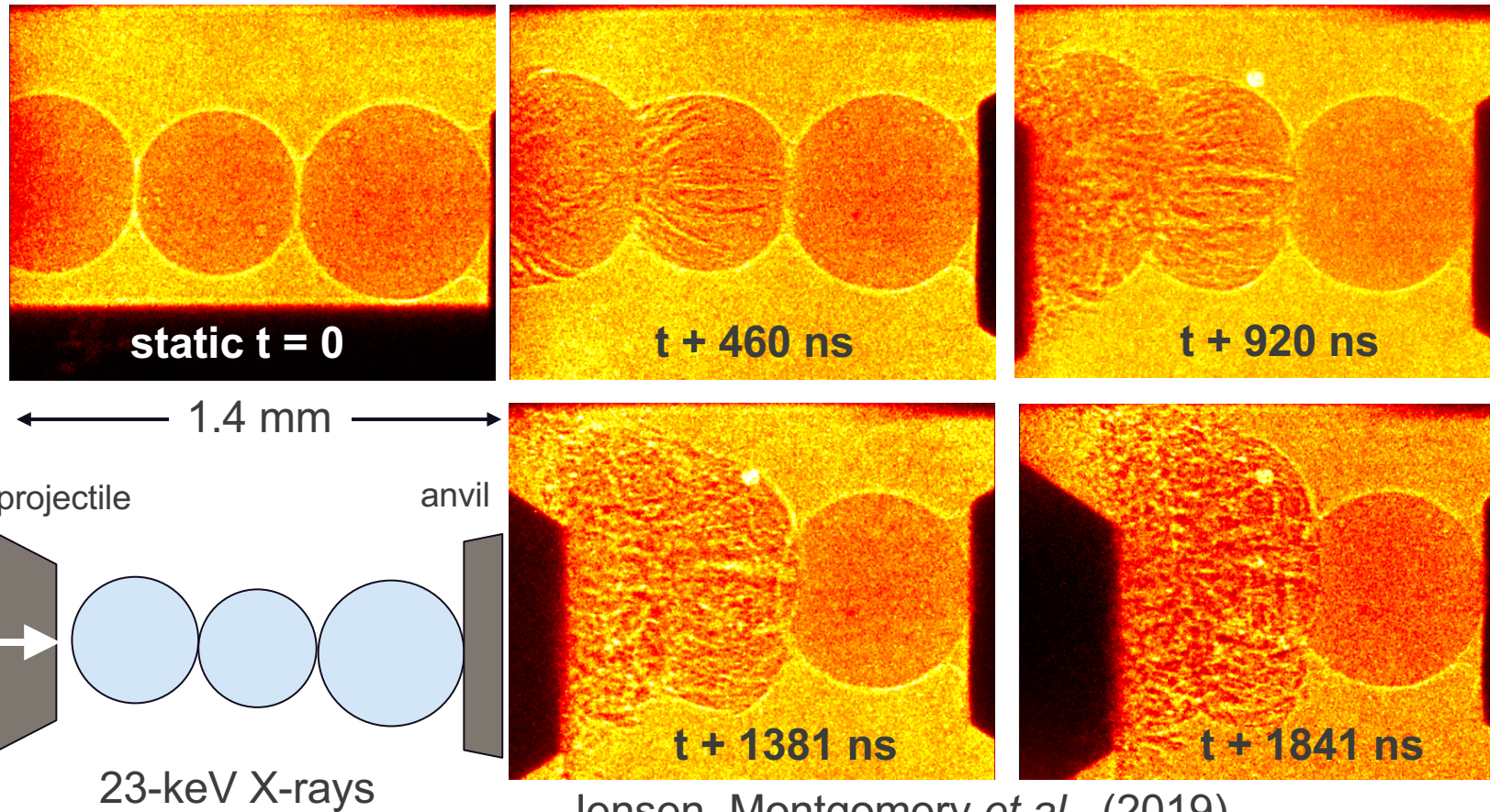
Jensen, Ramos, Yeager et al. (2013)

XPCI shows crack formation and propagation in vitreous carbon in APS synchrotron experiments

Ramos et al. (2013)

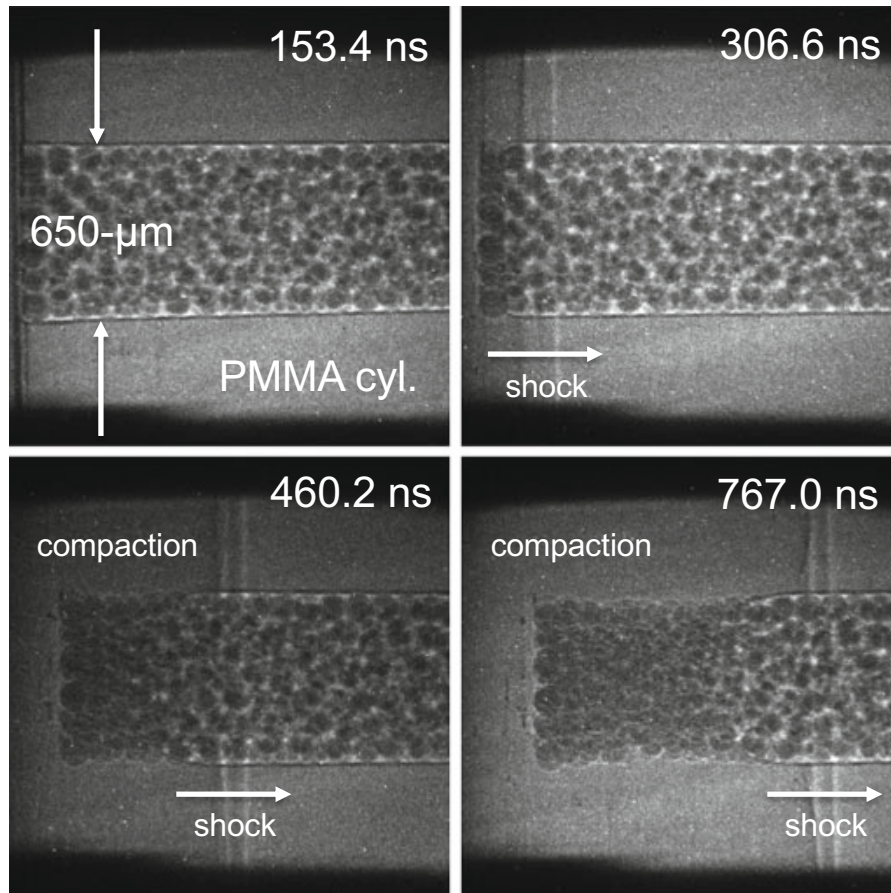


Four frame movie of Pyrex spheres impacted by steel projectile at ~ 240 m/s obtained with XPCI at APS



Jensen, Montgomery *et al.*, (2019)

XPCI is informing us about shock and compaction dynamics in granular and heterogeneous materials



- 104- μm Pyrex spheres packed in 650- μm diameter cylindrical bore of PMMA
- Cu flyer plate impactor from the left
- similar experiments on Martian and Lunar soil simulants (Regolith) were performed, and are being analyzed

Jensen, Montgomery et al. (2019)

Phase contrast imaging with neutrons?

- Many interesting objects are opaque to visible light, x-rays, but transparent to neutrons: How do you image them?

- neutron de Broglie wavelength (vacuum): $\lambda_0 = h/m_n v$

“thermal neutrons” $\lambda_0 \approx 1.8 \text{ \AA}$ $k_0 = 2\pi/\lambda_0 = \sqrt{2m_n E/\hbar}$

- neutron-nucleus potential: $V(\vec{r}) = 2\pi\hbar^2/m_n b\delta(\vec{r})$

$$\bar{V} = 2\pi\hbar^2/m_n \rho, \text{ where } \rho = \sum_i b_i N_i$$

- neutron obeys Schrödinger's equation: $[\nabla^2 + 2m(E - \bar{V})/\hbar^2]\psi(r) = 0$

$$k^2 = 2m(E - \bar{V})/\hbar^2 = k_0^2 - 4\pi\rho$$

$$n \equiv k/k_0 = 1 - \lambda_0^2 \rho / 2\pi$$

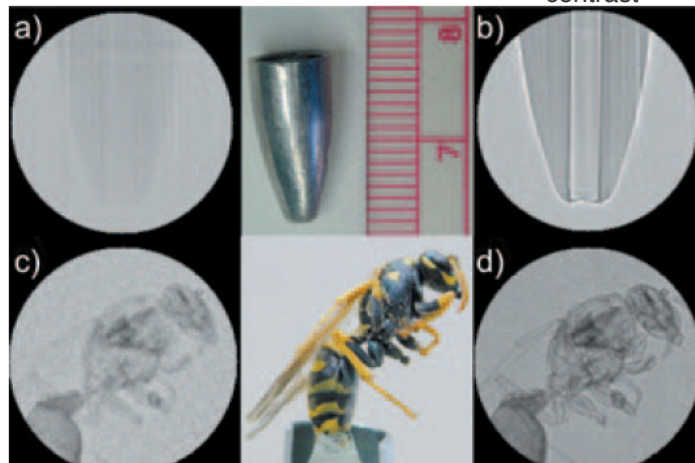
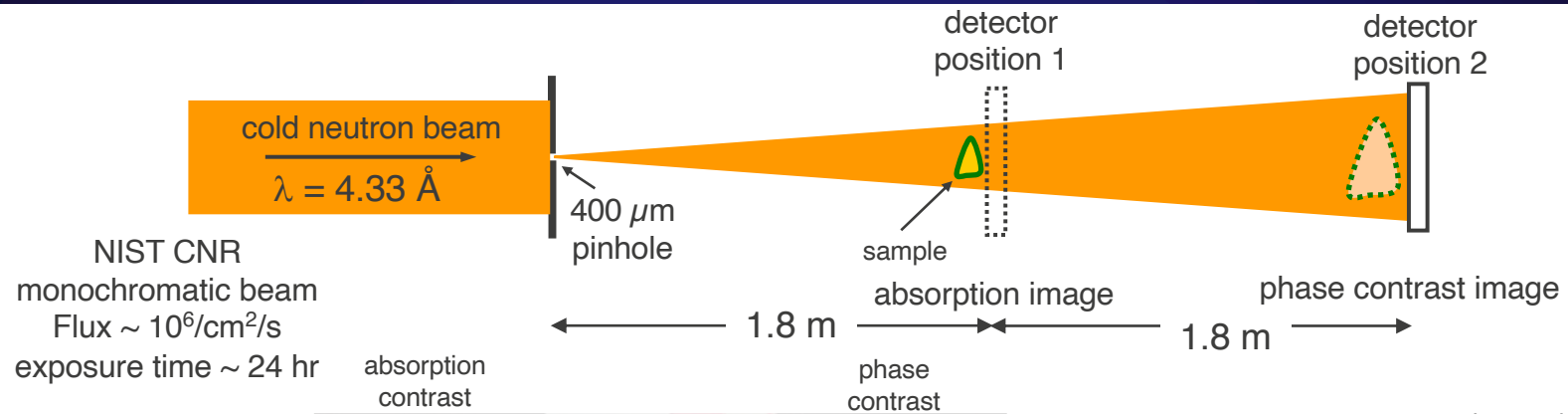
$$n = 1 - \delta + i\beta$$

Schrodinger Eq. reduces to
Helmholtz Eq. for optics

$$[\nabla^2 + k^2]\psi(r) = 0$$

same theory applies as for x-rays

Phase contrast imaging using neutrons was first performed by Allman et al. in 2000



B.E. Allman *et al.*, *Nature* **408**, 158 (2000)

Lehmann *et al.*, *NIMA* (2005)

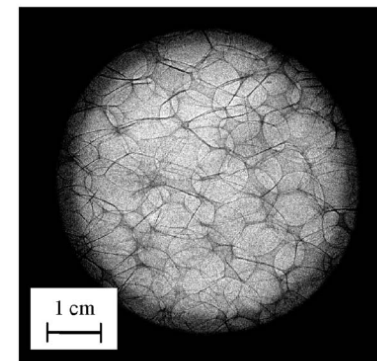


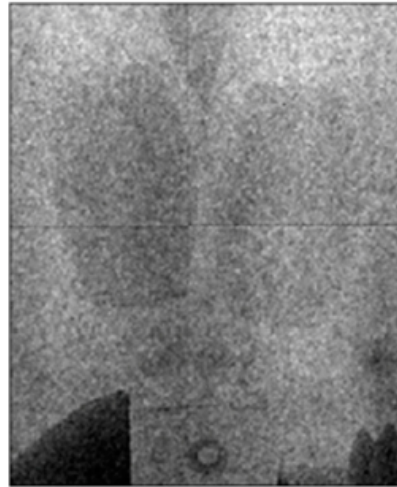
Fig. 3. Aluminium foam ($4 \times 4 \times 1 \text{ cm}$).

Neutron Phase Contrast Imaging was demonstrated with cold neutrons at LANSCE

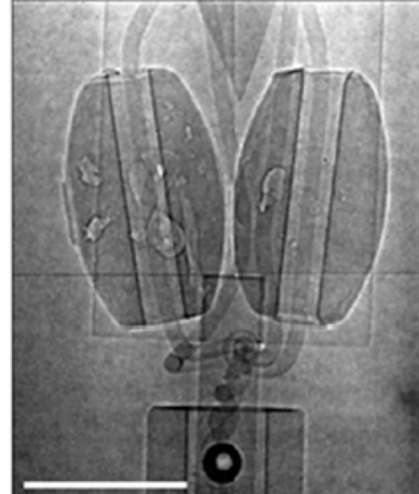
Pb sinkers & Al wire



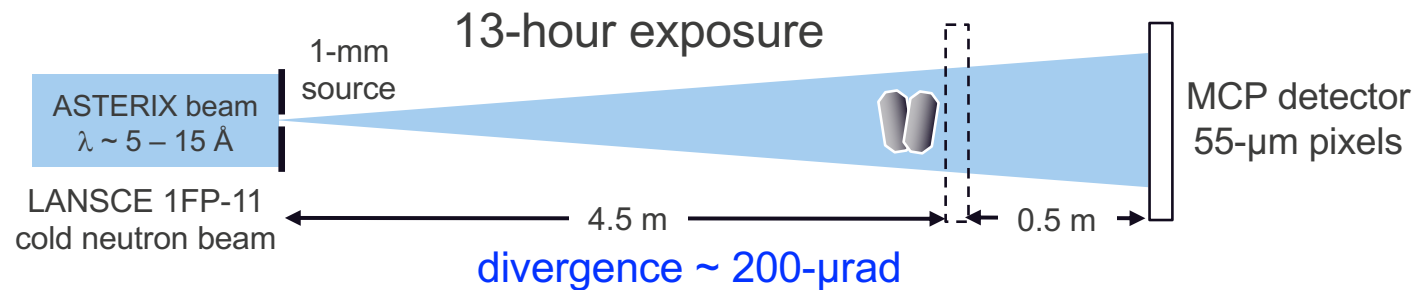
absorption contrast



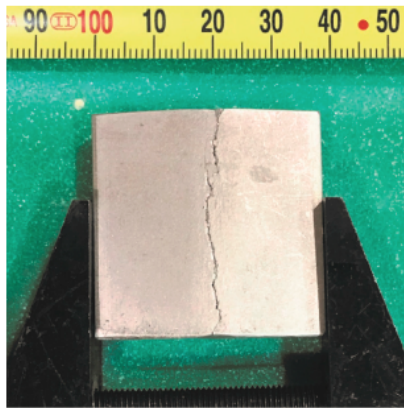
phase contrast



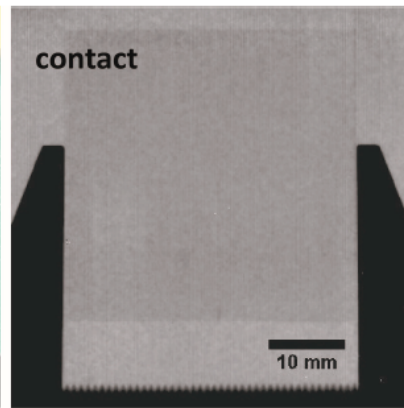
Nelson et al.,
J. Imaging (2018)



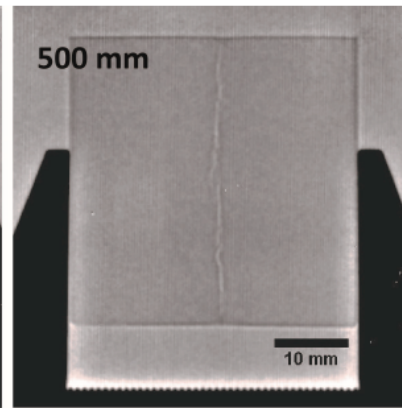
“Fast” neutron PCI is possible with relaxed spatial coherence and resolution at LANSCE



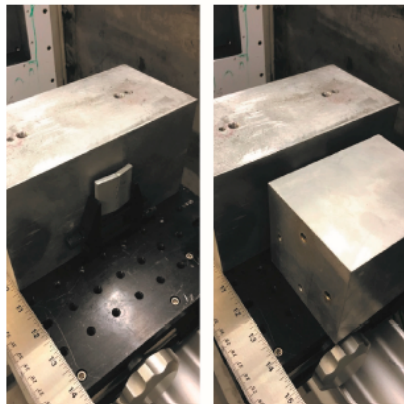
(a)



(b)

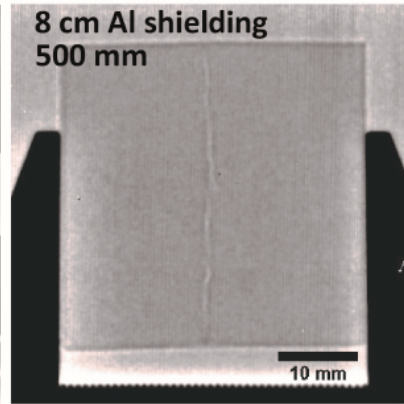


(c)

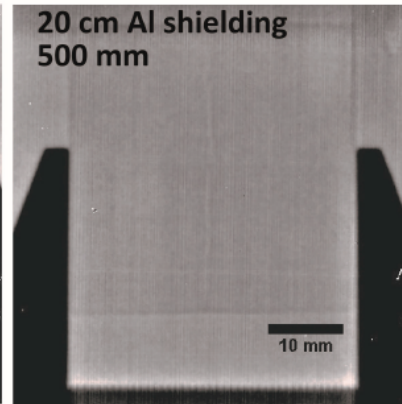


(d)

(e)



(f)



(g)

cracked Al sample:
4 cm x 4 cm x 0.5 cm
crack width ~ 150- μ m

Si flat panel detector
 6 Li:ZnS scintillator
127- μ m pixels

source: 5 mm aperture
(1 mRad divergence)
25x more flux
(10 – 30 min exposure)

source to object.: 4.5-m
object to detector: 0.5-m

**Nelson et al.,
J. Imaging (2018)**

Phase retrieval: approximations, ideal, general non-ideal

$$I_{ideal} = |\exp[i\varphi] * \exp[i\chi]|^2 \quad (\text{no noise, no blur, seldom applicable})$$

$$I_{non-ideal} = \wp\{\text{blur} * |\exp[i\varphi] * \exp[i\chi]|^2\} + \eta \quad (\text{noise, blur, general case})$$

- geometric optics or TIE regime: *linearize the propagator* $\exp[i\chi] \approx 1 + i\chi$
- CTF regime: *linearize the electric field* $\exp[i\varphi] \approx 1 + i\varphi$
- idealized general phase retrieval (exact, diffraction propagation, no noise/blur)
 - iterative methods (Gerchberg-Saxton, Fienup)
- non-ideal general phase retrieval (robust to noise, blur, use “super-resolution”)
 - image is noisy, blurry due to instrument resolution, finite beam divergence
 - often under-sampled in dynamic experiments (features \sim pixel size or smaller)
 - B. Wohlberg LDRD-DR on inverse problems

Phase retrieval in the geometric optics (TIE) regime has limited applicability for most of our experimental data

- geometric optics regime: small propagation distances

$$\exp[i\chi] = \cos(\chi) + i \cdot \sin(\chi) \approx 1 + i\chi$$

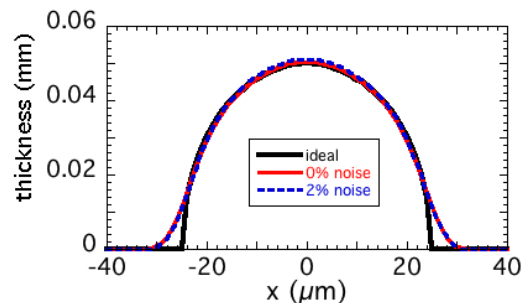
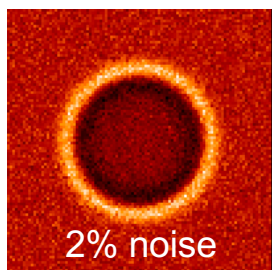
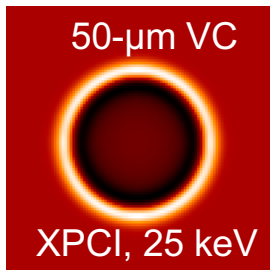
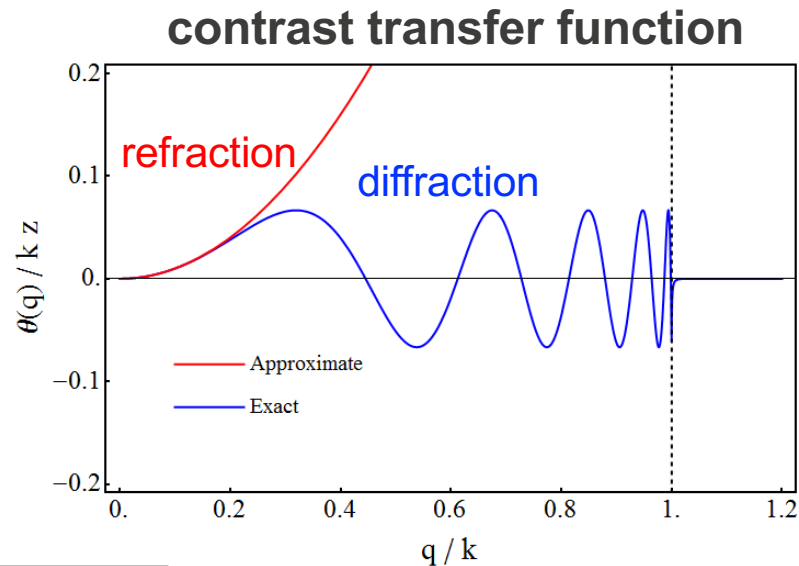
$$\chi = q^2 z/k \quad k = 2\pi/\lambda$$

pro: insensitive to noise

con: refraction only, limited range of use

when does $\sin(\chi) \approx \chi$? $z \leq \Delta x^2/2\lambda$

$\Delta x = 1.5\mu\text{m}, \lambda = 0.5\text{\AA} \rightarrow z \leq 22.5\text{mm}$



TIE retrieval for large z
*smooths out edges in
retrieved object*

CTF-based phase retrieval *can be exact* if linearization is applicable (weak phase object)

exit wave linearization: $\exp[i\varphi] \approx 1 + i\varphi$

valid *only* when: $\varphi \ll 1$ or $|\varphi(\mathbf{r} + \lambda z\mathbf{u}) - \varphi(\mathbf{r} - \lambda z\mathbf{u})| \ll 1$

$T=10 \mu\text{m}, \delta = 4\text{e-}7, \lambda = 0.5 \text{ \AA} \rightarrow \varphi \sim 0.5$ $z = 0.5 \text{ m}, \lambda = 0.5 \text{ \AA}, \Delta x = 1.5 \mu\text{m} \rightarrow \lambda z u \sim 8 \mu\text{m}$

CTF retrieval includes diffraction, refraction, absorption (*exact in linear limit*)

$$\hat{\varphi}(\mathbf{u}) = \frac{FFT[I/I_0 - 1]}{2\sin(\pi\lambda z\mathbf{u}^2) - 2\cos(\pi\lambda z\mathbf{u}^2)} = \frac{FFT[I/I_0 - 1]}{CTF(\mathbf{u}, \lambda, z)}$$

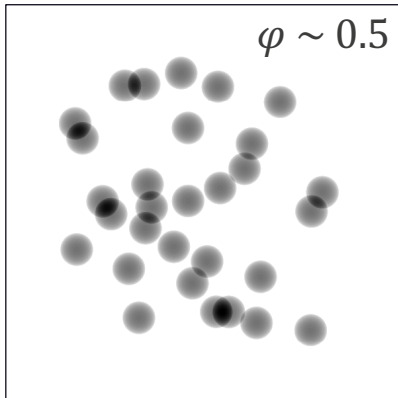
CTF has *zero crossings*, so even noiseless problem needs regularization

exciting possibility to include blur with regularization

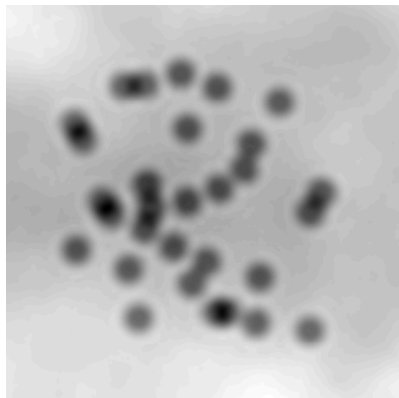
$$\hat{\varphi}(\mathbf{u}) = \frac{FFT[I/I_0 - 1]}{CTF(\mathbf{u}, \lambda, z) \cdot MTF(\mathbf{u})}$$

CTF phase retrieval with TGV-based regularization[†] looks extremely promising for this limited problem class

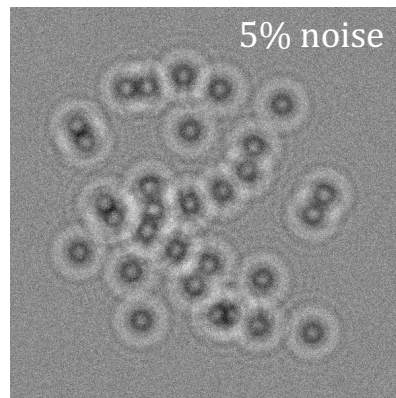
50- μm CH slab, 10- μm voids



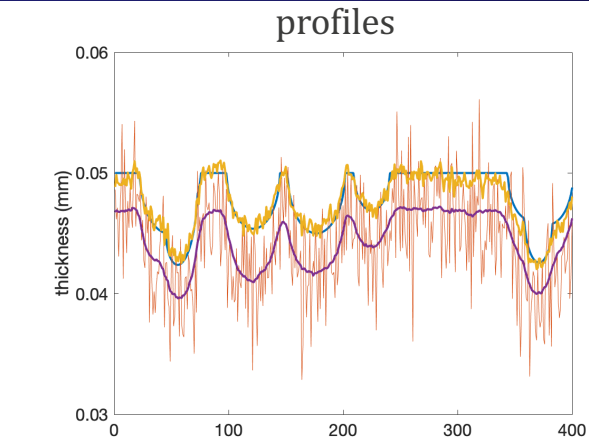
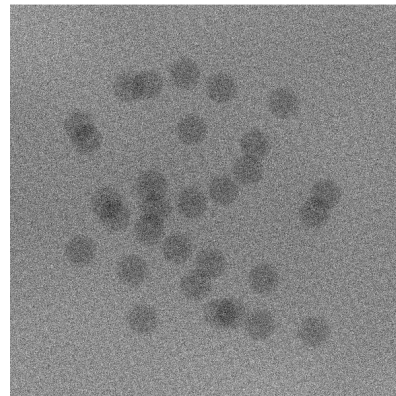
TIE retrieval



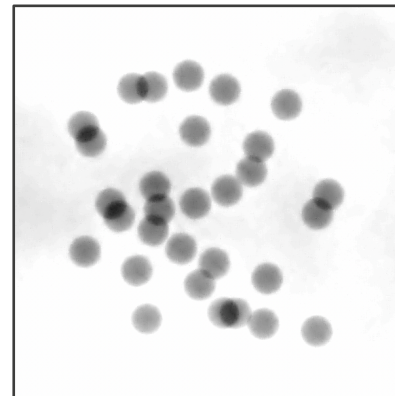
25 keV, $z = 100$ mm



CTF retrieval (Tik. reg.)



CTF retrieval (MHOTV reg.)

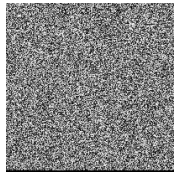


[†]Sanders *et al.*
 “Multiscale higher-order
 TV operators for L1 regularization”,
Adv. Struct. Chem. Imag. (2018)

Montgomery *et al.*
 in preparation (2021)

Iterative phase retrieval techniques rely on full wave propagation to converge to a phase solution

“initial guess”



ideal



$j^{\text{th}} + 1$ guess



“object plane”

“image plane”

forward propagate

apply “support” constraints

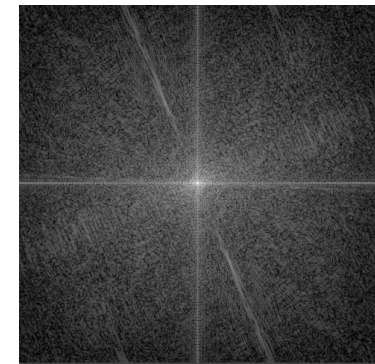
apply “modulus” constraints

$$A = \sqrt{I_m}$$
$$E'_i = A \cdot E_i / |E_i|$$

back propagate

measured intensity or diffraction pattern

I_m



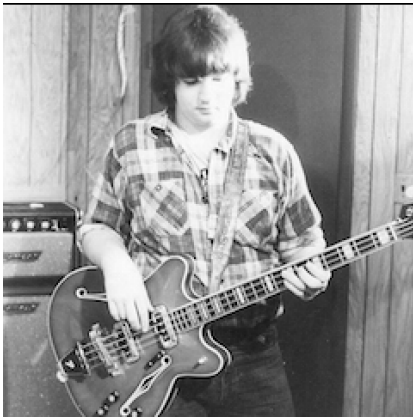
support constraints differentiate the various iterative algorithms, convergence

Gerchberg & Saxton (1972)
Fienup (1978)

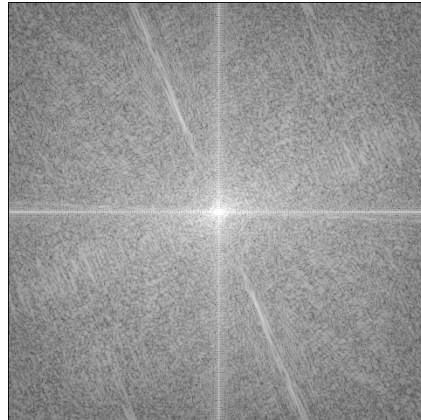
Hybrid Input-Output (HIO) algorithm[†] on idealized synthetic data shows slow numerical convergence

- demonstration in the far-field regime (FFT propagator)
- also possible in the near-field regime (Fresnel propagator)
- ideal case, no noise, no blur
- very slow to converge, takes 1000's of iterations

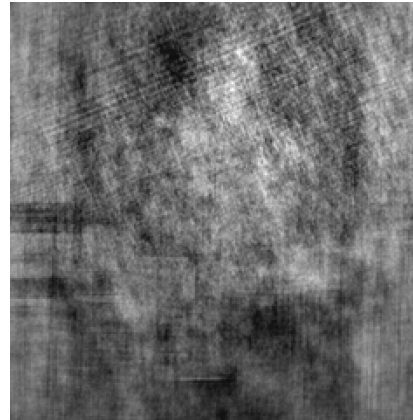
“phase object”



“measured image”



20 iterations

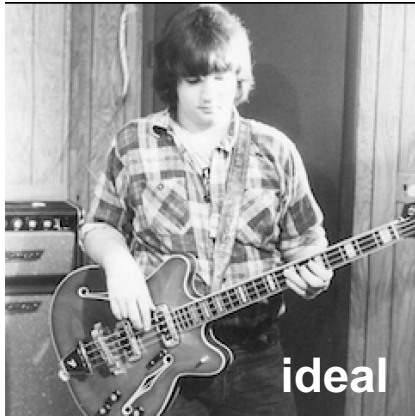


200 iterations



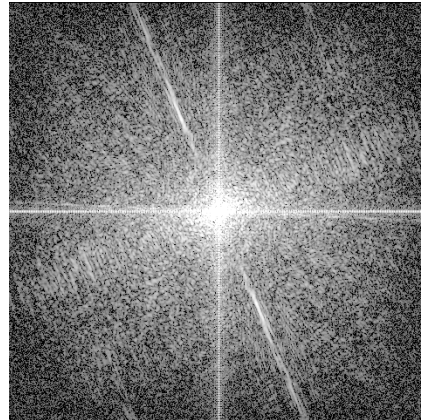
[†] Fienup (1978), (1982)

Iterative algorithms are extremely slow to converge in the presence of noise

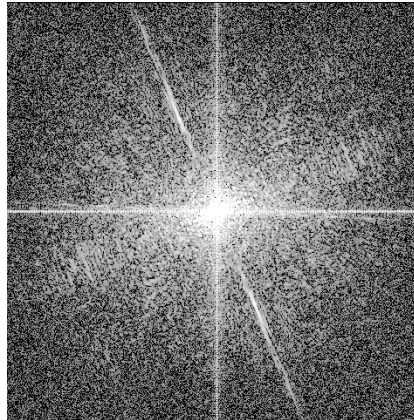


ideal

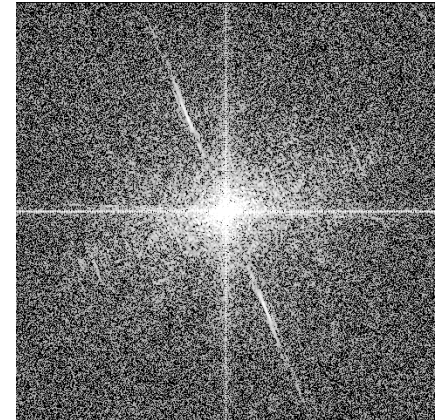
0% noise, $i=5000$



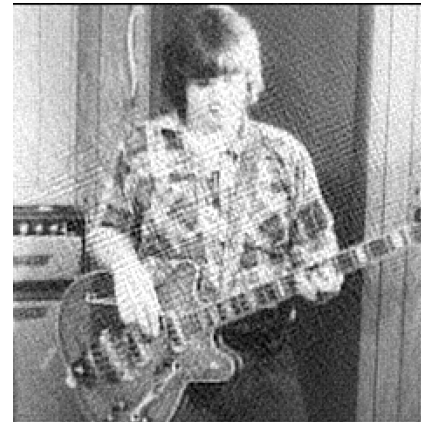
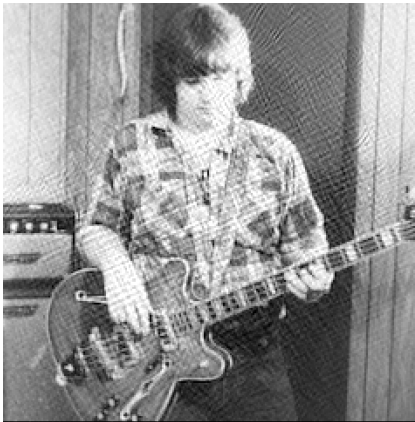
0.1% noise, $i=5000$



0.5% noise, $i=5000$



2% noise, 5000 iterations



Plans to hold an online course for propagation-based Phase Contrast Imaging

- Two day course (2 hour lectures each day)
- Day 1: cover propagation-based phase contrast imaging theory
 - image formation theory (geometric optics and scalar diffraction)
 - rules and guidelines for optimizing PCI setup in experiment
 - numerical forward modeling with scalar diffraction to predict image formation (will provide MatLab and IDL scripts)
- Day 2: quantitative phase retrieval techniques
 - geometric optics (TIE) phase retrieval
 - contrast transfer function (CTF) phase retrieval
 - iterative phase retrieval algorithms (Gerchberg-Saxton, Fienup, ...)
 - (will provide MatLab and IDL scripts)
- Tentatively in the April – May 2021 time frame

Summary and Conclusions

- propagation-based phase contrast imaging
 - does not require specialized optics
 - does not require monochromatic source (broad band source okay)
 - only requires sufficient spatial coherence
- first application of XPCI to dynamic experiments by LANL
- applied to cold neutron sources at LANSCE and elsewhere
- can be quantitative, similar to absorption-based imaging
 - phase \sim projected areal density, same as absorption-based imaging
- Advertisement for phase contrast imaging class